of **2**, free CH_3CN (1.97 ppm), and Et_2O (3.49 (q), 1.15 (t)), the resonances for **3** were observed. ^1H NMR (CD_2Cl_2): δ 7.51 (m, P-Ph), 2.31 (s, CH_3CN), 1.63 (d, P-Me, J_{PH} = 8 Hz), -10.02 (q, Os-H, J_{PH} = 4 Hz).

Kinetic Studies. In the glovebox, 225 mg (0.37 mmol) of OsH_4P_3 was weighed and dissolved in 2.0 mL of CH_2Cl_2 (0.19 M). Under N_2 purge, 80 μL of $HBF_4 \cdot OEt_2$ (0.82 mmol) was added. The excess was employed to ensure production of only **3** and **6** (singlets in ^{31}P); the A_2B pattern of **4** would be more difficult to integrate. The above solution was transferred to two NMR tubes (0.5 mL each). To the first was added 110 μL of a 4:1 CH_2Cl_2/CH_3CN solution (0.42 mmol of CH_3CN, 0.69 M), and the reaction was monitored via $^{31}P\{^1H\}$ NMR (20 °C). To the second tube was added 110 μL of neat CH_3CN (2.12 mmol of CH_3CN, 3.5 M), and the reaction was monitored similarly. Both reactions lasted 1-1.5 h, and spectra were recorded (15 s acquisition time) every 5-10 min. The rate of disappearance of **2** exhibited first-order behavior and the rate constant k_{obsd} ($\equiv k_1$, eq 9) was determined as the slope of a plot of ln $[(\mathbf{2})_0/(\mathbf{2})_t]$ vs. time; data are given in Table IV.

Acknowledgment. This work was supported by Dow Chemical Corp. and by the Bloomington Academic Computing System. The deuterium NMR spectra were obtained on an instrument funded in part by NSF Grant No. CHE-80-05004.

Registry No. 1, 24228-57-7; **2** (BF_4), 88703-91-7; **3** (BF_4), 88703-93-9; **4** (BF_4), 88703-95-1; **5**, 88764-07-2; **6** $(PF_6)_2 \cdot CH_2Cl_2$, 88703-96-2; **6** $(PF_6)_2$, 88703-89-3; **6** $(BF_4)_2$, 88129-95-7; $HBF_4 \cdot OEt_2$, 67969-82-8; Ph_3CPF_6, 437-17-2; CH_3CN, 75-05-8.

Supplementary Material Available: Anisotropic temperature factors, distances and angles within the PMe_2Ph, PF_6^-, and CH_2Cl_2 moieties, and observed and calculated structure factors for $[Os(NCMe)_3(PMe_2Ph)_3](PF_6)_2 \cdot CH_2Cl_2$ (36 pages). Ordering information is given on any current masthead page.

Structural Phase Transitions in Dihalo(*N*,*N*′-disubstituted-diazabutadiene)nickel Complexes. Structures of Bis[dibromo(*N*,*N*′-di-*tert*-butyldiazabutadiene)nickel] and Dibromo(*N*,*N*′-di-*tert*-butyldiazabutadiene)nickel

Geoffrey B. Jameson,*† Hans Rudolf Oswald,‡ and Hans Rudolf Beer‡

Contribution from the Department of Chemistry, Georgetown University, Washington, DC 20057, and the Institute of Inorganic Chemistry, University of Zürich, 8057 Zürich, Switzerland.
Received April 25, 1983

Abstract: Violet tetrahedral complexes $NiX_2(dab)$ (X = Br, Cl; dab = *N*,*N*′-disubstituted-diazabutadienes) are formed when crystals of the yellow dimers $[NiX_2(dab)]_2$ are heated. The structural transformation when X = Br and dab = *N*,*N*′-di-*tert*-butyldiazabutadiene is irreversible but topotactic—single crystallinity is largely preserved in the transformation. The yellow complex has been found by single-crystal X-ray structure analysis to be a distorted trigonal-bipyramidal centrosymmetric dimer: Ni-Br(terminal) = 2.457 (1) Å, Ni-Br(bridging) = 2.497 (1) and 2.583 Å, Ni-N = 2.042 (4) and 2.039 (4) Å, Br(terminal)-Ni-Br(bridging, long) = 165.79 (3)° (defines the pseudotrigonal axis), Br(bridging)-Ni-Br(bridging) = 83.11 (3)°, N-Ni-N = 80.8 (2)°. The monomer (structural analysis of a sample separately prepared at ~130 °C) has tetrahedral D_{2h} symmetry: Ni-Br = 2.333 (2) and 2.343 (2) Å, Ni-N = 1.996 (7) and 2.002 (8) Å, Br-Ni-Br = 126.78 (6)°, N-Ni-N = 82.5 (3)°. The reaction mechanism involves cleavage of the long Ni-Br bond and concerted movement of $NiBr_2(dab)$ monomers with concomitant rearrangement to a tetrahedral D_{2d} system such that centrosymmetrically related Ni centers, formerly 3.806 Å separated, become separated by 9.893 Å and related by a 2_1 screw axis. Movements of the monomeric $NiBr_2(dab)$ units of about 10 Å are observed, while crystallinity is largely preserved. Relevant crystal and refinement data are as follows. For $[NiBr_2(dab)]_2$: space group C_{2h}^6-$C2/c$, a = 20.429 (5) Å, b = 7.156 (1) Å, c = 20.504 (5) Å, β = 98.50 (2)°, V = 2965 Å^3 at 22 °C, Z = 4 (dimers have $\bar{1}$ symmetry), ρ_{calcd} = 1.73, ρ_{obsd} = 1.72 (1) g/cm^3, 2560 reflections with $I > 3\sigma_I$ in the range $0.0246 < (\sin\theta)/\lambda < 0.7049$ Å^{-1} (graphite-monochromated Mo Kα radiation), R and R_w on F 0.039 and 0.047. For $NiBr_2(dab)$: space group C_{2h}^5-$P2_1/n$, a = 7.125 (3) Å, b = 19.717 (10) Å, c = 10.396 (5) Å, β = 90.91 (2)°, V = 1459 Å^3 at -150 °C, Z = 4, ρ_{calcd} = 1.67, ρ_{obsd} = 1.66 (1) g/cm^3 (based upon room-temperature cell constants), 2300 reflections in the range $0.0246 < (\sin\theta)/\lambda < 0.5734$ Å^{-1}, R and R_w on F^2 (all data including $F^2 < 0$ was used) 0.091 and 0.127, for the 1545 reflections with $I > 3\sigma_I$ R and R_w on F 0.055 and 0.062.

The evaluation of kinetic parameters for solid-state reactions and structural phase transitions is conventionally based on analogy to the theory for processes occurring in homogeneous solution for lack of any better formulation.[1] Thus, when free mobility of particles can no longer occur, when temperature exchange between the reacting species and solvent is not relevant, and when physical meaning for the reaction order is absent, interpretation of kinetic parameters is hazardous. Nonetheless by taking a series of compounds of known structure and comparing the parameters derived, it should be possible to make some meaningful comparisons and interpretations. In order to relate kinetic and thermodynamic data to a *mechanism* for the solid-state reaction or structural transformation, these processes should occur topotactically.[2,3] For only with knowledge of the crystallographic

†Georgetown University.
‡University of Zürich.

(1) (a) Sestâk, J.; Satava, V.; Wendlandt, W. W. *Thermochim. Acta* **1973**, *7*, 333-352. (b) Behnisch, J.; Schaff, E.; Zimmermann, H. *J. Therm. Anal.* **1978**, *13*, 117-128. (c) Coats, A. W.; Redfern, J. P. *Nature (London)* **1964**, *201*, 68-69. (d) Satava, V. *Thermochim. Acta* **1971**, *2*, 423-428.

(2) Following Günter and Oswald,[3a] we define a reaction as topotactic if the solid product is formed in one or only several definite crystallographic orientations relative to the parent crystal as a consequence of a chemical reaction or solid-state structural transformation and if it can proceed throughout the entire volume of the parent crystal. This definition differs in words only from several others.

0002-7863/84/1506-1669$01.50/0

Table I. Data Collection Details for I and II

	$[NiBr_2(dab)]_2$ (I)	$NiBr_2(dab)$ (II)
empirical formula	$NiBr_2C_{10}H_{20}N_2$	$NiBr_2C_{10}H_{20}N_2$
formula weight, amu	386.81	386.81
space group	C_{2h}^6-$C2/c$	C_{2h}^5-$P2_1/n$
a, Å	20.429 (5)	7.125 (3)
b, Å	7.156 (1)	19.717 (10)
c, Å	20.504 (5)	10.396 (5)
β, deg	98.50 (2)	90.91 (2)
V, Å^3	2965	1459
Z	8	4
ρ_{obsd}, ρ_{calcd}, g cm^{-3}	1.72 (1), 1.73	1.66 (1), 1.67[a]
temperature, °C	22	−150
radiation	graphite-monochromated Mo $K\alpha_1$ (λ = 0.7093 Å)	
crystal shape	elongated, parallelepiped	flattened needle
	~0.49 × 0.22 × 0.20 mm	~0.22 × 0.14 × 0.06 mm
crystal volume, mm^3	0.024	0.0022
linear abs coeff, cm^{-1}	66.31	67.37
transmission factors	0.15–0.36	0.40–0.69
detector aperture	4.8 mm wide, 4.8 mm high	5.8 mm wide, 4.6 mm high
take-off angle, deg	2.2	2.1
scan speed	2.0° in 2θ per min for $\lambda^{-1}\sin\theta < 0.6401$ Å^{-1}; 1.0° per min otherwise	2.0° in 2θ per min;[b] rescan option used
$\lambda^{-1}\sin\theta$ limits, Å^{-1}	0.0246–0.7049	0.0369–0.5734
background counts	initially 10 s at each end of scan, then 20 s	10 s at each end of scan[b]
scan range	1.0° in 2θ below $K\alpha_1$ to 1.0° above $K\alpha_2$	
data collected	$\pm h,-k,l, h \pm k$ odd omitted	$\pm h,k,-l$
unique data collected	4355	2300
unique data with $F_o^2 > 3\sigma(F_o^2)$	2560	1545

[a] Based on room-temperature unit cell: a = 7.166 Å; b = 20.359 Å, c = 10.508 Å, β = 91.03°, V = 1533 Å^3. [b] Lenhert, P. G. *J. Appl. Crystallogr.* 1975, *8*, 568–570.

relationships between the parent crystal and its product may it become possible to deduce how atoms or groups of atoms move relative to one another.

Topotatic processes are widely known among strictly inorganic compounds (for reviews see ref 3a–c); but coordination compounds displaying these phenomena are relatively rare (or at least less studied). Several types of solid-state reaction may be defined. In order of increasing complexity of the stereochemical reorganization, they are simple structural phase transitions (e.g., order–disorder transitions[4]), isomerization reactions (e.g., coordination nitrito → nitro[5]), oligomerization–deoligomerization reactions,[3d,6] and reactions involving the exchange of ligand or solvent/solvate molecules with the environment.[7] Of the latter reactions few have been unambiguously characterized as topotactic through single-crystal diffractometry, although some well-known intercalation reactions, characterized by using polycrystalline materials, may be topotactic.[8] For wholly organic systems a number of topotactic photochemical[9a,b] and thermal[9c] oligomerization reactions have been described, and many topochemical processes are known.[9d] Topotactic processes are distinguished from topochemical processes by the additional requirements that the crystal structure of the product maintain specific crystallographic orientation(s) relative to the crystal structure for the starting material.[2]

With the system $NiX_2(dab)$, X = Cl or Br and dab = *N,N'*-disubstituted-diazabutadiene, we have been able to study in detail the structural phase transition or deoligomerization reaction from distorted trigonal-bipyramidal dimers to tetrahedral monomers. A preliminary report on some of the thermoanalytical data has already been presented.[10]

Experimental Section

Preparation of *N,N'*-Di-*tert*-butylethylenedilimine (dab). At 0 °C, 36.3 g (0.25 mol) of 40% glyoxal in water was added dropwise with stirring to 36.7 g (0.5 mol) of *tert*-butylamine. The solution was stirred for 2 h. The white solid was separated by filtration and dissolved in ether, and the solution was dried over $MgSO_4$. The solution was concentrated, and the product crystallized upon cooling to −80 °C (yield 28.4 g, 0.17 mol, 68%; mp 43.0–44.1 °C (lit.[11a] mp 39–43 °C)); analysis for $C_{10}H_{10}N_2$, obsd (calcd): C, 71.03 (71.37); H, 12.18 (11.98); N, 16.65 (16.85)). Other *N,N'*-disubstituted ligands were similarly prepared.

Preparation of $[NiBr_2(dab)]_2$ (I). Dibromodimethoxyethanenickel (6.0 g, 19.4 mmol[11b]) was mixed with 2.9 g (17 mmol) of dab in 50 mL of acetone and stirred for 2 h. Upon concentration, 6.4 g (16.6 mmol, 98% yield) of I was isolated by filtration. The material was recrystallized from CH_2Cl_2 to yield large yellow-brown weakly hygroscopic needles; analysis for $C_{10}H_{10}N_2NiBr_2$, obsd (calcd): C, 30.87 (31.05); H, 5.14 (5.21); N, 7.55 (7.24); Ni, 15.12 (15.18). Diffraction-quality crystals were obtained with difficulty by slow evaporation of a toluene solution of I or by slow growth of crystals in a temperature gradient (convective crystallization). Other complexes with chloro and other dab ligands were similarly prepared.

(3) (a) Oswald, H. R.; Günter, J. R. "Crystal Growth and Materials"; Kaldis, E., Scheel, H. J., Eds.; North-Holland Publishing Co.: Amsterdam, 1977; p 416. (b) Günter, J. R.; Oswald, H. R. *Bull. Inst. Chem. Res. Kyoto Univ.* **1975**, *53*, 249–255. (c) Dent Glasser, L. S.; Glasser, F. P.; Taylor, H. F. W. *Q. Rev., Chem. Soc.* **1962**, *16*, 343–360. (d) Cheng, K.; Foxman, B. M. *J. Am. Chem. Soc.* **1977**, *99*, 8102–8103.

(4) For example: (a) Seiler, P.; Dunitz, J. D. *Acta Crystallogr., Sect. B* **1979**, *B35*, 2020–2032. (b) Jameson, G. B.; Schneider, R.; Dubler, E.; Oswald, H. R. *Ibid.* **1982**, *B38*, 3016–3020.

(5) For example: (a) Grenthe, I.; Nordin, E. *Inorg. Chem.* **1979**, *18*, 1109–1116. (b) Grenthe, I.; Nordin, E. *Ibid.* **1979**, *18*, 1869–1875.

(6) For example: (a) Walton, R. A.; Whyman, R. *J. Chem. Soc. A* **1968**, 1394–1398. (b) Drew, M. G. B.; Lewis, D. F.; Walton, R. A. *J. Chem. Soc., Chem. Commun.* **1969**, 326. (c) Snow, M. R.; Boomsma, R. F. *Acta Crystallogr., Sect. B* **1972**, *B28*, 1908–1913. (d) Clarke, P. J.; Milledge, H. J. *Ibid.* **1975**, *B31*, 1543–1553. (e) Clarke, P. J.; Milledge, H. J. *Ibid.* **1975**, *B31*, 1554–1558. (f) Long, G. J.; Bertrand, G. L.; Noel, D.; Wu, S. H.; Mayhan, K. G.; Coffen, D. L. *J. Chem. Soc., Dalton Trans.* **1975**, 762–765.

(7) For example: (a) Bachmann, W.; Jameson, G. B.; Dubler, E.; Oswald, H. R., to be published. (b) Reller, A. R.; Oswald, H. R., to be submitted. (c) Jameson, G. B.; Molinaro, F. S.; Ibers, J. A.; Collman, J. P.; Brauman, J. I.; Rose, E.; Suslick, K. S. *J. Am. Chem. Soc.* **1980**, *102*, 3224–3237.

(8) (a) Johnson, J. W.; Jacobson, A. J.; Rich, S. M.; Brody, J. F. *J. Am. Chem. Soc.* **1981**, *103*, 5246–5247. (b) Johnson, J. W.; Jacobson, A. J.; Brody, J. F.; Rich, S. M. *Inorg. Chem.* **1982**, *21*, 3820–3825. (c) Walker, G. F.; Hawthorne, D. G. *Trans. Faraday Soc.* **1967**, *63*, 166–174.

(9) (a) Wilson, R. B.; Duesler, E. N.; Curtin, D. Y.; Paul, I. C.; Baughman, R. H.; Preziosi, A. F. *J. Am. Chem. Soc.* **1982**, *104*, 509–516. (b) Nakanishi, H.; Jones, W.; Thomas, J. M.; Hursthouse, M. B.; Motevalli, M. *J. Phys. Chem.* **1981**, *85*, 3636–3642. (c) Wilson, R. B.; Chin. Y.-S.; Paul, I. C.; Curtin, D. Y. *J. Am. Chem. Soc.* **1983**, *105*, 1672–1674.

(10) Beer, H. R.; Oswald, H. R. *Proc. VI Int. Conf. Thermal Anal.* **1980**, 121–125.

(11) (a) Kliegman, J. M.; Barnes, R. K. *Tetrahedron* **1970**, *26*, 2555–2560. (b) King, R. B. "Organometallic Syntheses"; Academic Press: New York, 1965; Vol. I.

Table II. Final Atomic Parameters for $[NiBr_2(dab)]_2$

atom	x	y	z	U_{11}[a]	U_{22}	U_{33}	U_{12}	U_{13}	U_{23}
Ni	0.24197 (3)	0.18088 (8)	0.08797 (3)	6.29 (4)	2.88 (3)	2.98 (3)	−0.12 (3)	1.05 (2)	0.26 (2)
Br(1)	0.23640 (3)	0.36309 (8)	0.18859 (2)	11.84 (5)	3.48 (3)	4.07 (3)	−0.16 (3)	2.58 (3)	−0.43 (2)
Br(2)	0.27717 (3)	0.46060 (7)	0.02919 (2)	12.18 (5)	3.84 (3)	3.24 (2)	−2.25 (3)	1.63 (3)	−0.03 (2)
N(1)	0.1788 (2)	−0.0134 (6)	0.1167 (2)	5.36 (24)	3.90 (21)	3.02 (16)	−0.08 (20)	0.62 (16)	−0.18 (16)
N(2)	0.3095 (2)	−0.0133 (6)	0.1274 (2)	5.91 (26)	4.15 (22)	3.15 (17)	0.46 (21)	1.08 (17)	−0.21 (17)
C(1)	0.2091 (3)	−0.1525 (7)	0.1433 (2)	6.63 (34)	3.61 (24)	4.45 (24)	−0.93 (25)	1.40 (24)	0.42 (21)
C(2)	0.1052 (3)	−0.0042 (9)	0.1115 (2)	5.83 (34)	6.78 (38)	4.81 (27)	−0.15 (32)	0.45 (25)	0.53 (28)
C(3)	0.0868 (3)	0.0050 (14)	0.1800 (3)	8.07 (46)	15.4 (8)	6.90 (40)	2.31 (53)	3.01 (35)	1.78 (49)
C(4)	0.0826 (3)	0.1718 (14)	0.0742 (4)	6.70 (46)	15.1 (9)	14.2 (7)	2.41 (54)	2.11 (47)	7.56 (69)
C(5)	0.0750 (4)	−0.1704 (16)	0.0749 (5)	8.02 (56)	16.2 (10)	19.1 (10)	−3.87 (64)	0.09 (59)	−7.08 (87)
C(6)	0.2810 (3)	−0.1529 (7)	0.1487 (2)	6.86 (34)	3.11 (24)	3.91 (22)	0.56 (24)	0.92 (23)	0.73 (19)
C(7)	0.3829 (3)	−0.0051 (9)	0.1334 (3)	5.57 (34)	5.88 (35)	6.10 (31)	0.76 (30)	1.47 (26)	1.19 (28)
C(8)	0.3985 (4)	0.0081 (15)	0.0645 (4)	8.41 (47)	17.7 (9)	8.43 (47)	2.14 (57)	4.17 (39)	2.39 (57)
C(9)	0.4026 (4)	0.1693 (17)	0.1696 (6)	5.56 (47)	19.5 (12)	29.7 (14)	−3.35 (62)	2.84 (64)	−15.2 (11)
C(10)	0.4168 (4)	−0.1715 (16)	0.1671 (5)	6.74 (49)	17.4 (11)	21.4 (11)	3.96 (59)	3.56 (58)	11.5 (9)

[a] The form of the anisotropic thermal ellipsoids is $\exp[-2\pi^2(U_{11}h^2a^{*2} + U_{22}k^2b^{*2} + U_{33}l^2c^{*2} + 2U_{12}hka^*b^* + 2U_{13}hla^*c^* + 2U_{23}klb^*c)]$. Values are multiplied by 100.

Preparation of $NiBr_2$(dab) (II). This was prepared analogously to I except that nitrobenzene solution, saturated at room temperature, was slowly evaporated in an oven at 130 °C to yield violet crystals (the essentially irreversible yellow → violet transformation occurs at 105 °C in the solid state).

In both cases the single crystals selected for data collection were demonstrated to be representative of the bulk sample by powder photography.

Crystallographic Study of $[Ni(dab)Br_2]_2$ (I, Yellow Form). Since crystals were moderately unstable with respect to atmospheric moisture, they were sealed in thin-walled capillaries. Crystals of suitable quality were very few. Monoclinic symmetry and systematic absences consistent with the space groups Cc or $C2/c$ were observed by precession and Weissenberg photography. Diffraction data were collected with a Picker FACS-I diffractometer. Optimal lattice parameters and crystal orientation were obtained by least-squares refinement of the setting angles of 12 automatically centered reflections in the range $0.4252 < \lambda^{-1} \sin\theta < 0.4903$ Å^{-1}. Other data collection details are summarized in Table I. Midway through data collection the crystal moved; its orientation was then redetermined. Otherwise the intensities of three standard reflections monitored regularly showed no significant variation.

The structure was solved by conventional heavy-atom Patterson methods and developed through cycles of full-matrix least-squares refinement interspersed with Fourier syntheses. The XRAY72 program package as implemented with the ETH-Zurich CDC system was used. Isotropic refinement converged at rather discouraging values for R and R_w of 0.217 and 0.170. However, upon relaxation of the constraints on thermal motion these values decreased to 0.047 and 0.043 after four cycles. Hydrogen atoms were located in a difference Fourier synthesis and included as a fixed contribution to F_c at their idealized positions (C–H = 0.95 Å, C–C–H = 109.5° for methyl hydrogen atoms).

After a further two cycles the weighting scheme was optimized [$w = 1/(\sigma^2\text{counting}) + 0.0003(F_o)^2$)] so that the minimized function $\sum w(|F_o| - |F_c|)^2$ was independent of the magnitude of F_o and $\lambda^{-1} \sin\theta$. Refinement converged at values for R and R_w of 0.039 and 0.047. The final value for the standard error in an observation of unit weight is 1.74 e. The final difference Fourier was flat and featureless.

Table II lists atomic parameters for non-hydrogen atoms, Table III hydrogen atom parameters, and Table IV $10|F_o|$ vs. $10|F_c|$. The latter two tables are available as supplementary material.

Crystallographic Study of Ni(dab)Br_2 (II, Violet Form). Monoclinic symmetry and systematic absences uniquely consistent with the space group $P2_1/n$ (x, y, z; $^1/_2 + x, ^1/_2 - y, ^1/_2 + z$; $-x, -y, -z$; $^1/_2 - x, ^1/_2 + y, ^1/_2 - z$) were observed by methods similar to those for I. Pronounced pseudomirror symmetry between hkl and $hk\bar{l}$ reflections was noticed for II. After much searching for a suitable crystal, diffraction data were eventually collected in a manner similar to before, but with a modified Nonius low-temperature device. Optimal lattice parameters and cell constants were obtained by the least-squares refinement of the setting angles of 20 automatically centered reflections in the range $0.2533 < \lambda^{-1} \sin\theta < 0.3470$ Å^{-1}. Other data collection parameters may be found in Table I. Early in data collection the crystal moved; its orientation was redetermined. Standards showed no significant variation during the course of data collection.

The structure was solved and refined as before except that all calculations were done upon the University of Zürich's IBM3033 computer using a modified version of the Northwestern University crystallographic computing library.[12] Hydrogen atoms were located and included as a fixed contribution to F_c at their idealized positions. Because the crystal was rather small and did not diffract strongly, in the final cycles of least-squares refinement all data (including $F^2 < 0$) were used. At convergence the values of R and R_w (on F^2) were 0.091 and 0.127; the final value for the standard error in an observation of unit weight was 1.26 e^2. For the portion of the data where $F^2 > 3\sigma(F^2)$, the values for R and R_w were 0.055 and 0.062. The weighting scheme based upon data originally processed with a p factor of 0.04 was satisfactory ($1/w = \sigma^2 = (S + (B_1 + B_2)(t_S/t_B)^2 + (pI)^2)$, where S is the raw intensity, B_1 and B_2 are background counts, t_S is the scan time, t_B is the time for an individual background measurement, and I is the net intensity). Notwithstanding the high temperature at which crystals were grown, crystal quality was adequate and the final difference Fourier map was flat and featureless.

Table V lists atomic parameters for non-hydrogen atoms, Table VI hydrogen atom parameters, and Table VII $10|F_o|$ vs. $10|F_c|$. A negative entry denotes a reflection for which $F^2 < 0$. The latter two tables are available as supplementary material.

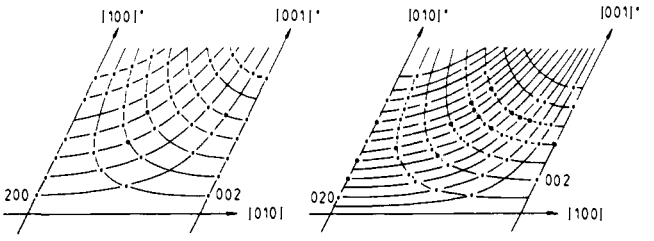

Figure 1. Diagrammatic representation of the Weissenberg photograph of yellow $[NiBr_2(dab)]_2$ before (left) and after (right) the transformation at 105 °C to the violet $NiBr_2$(dab).

Chart I

$[NiBr_2(dab)]_2$ (yellow)		$NiBr_2$(dab) (violet)
(100)	parallel	(010)
(010)	parallel	(100)
[100]	approx parallel	[010] (angle change of 8.5°)
[010]	approx parallel	[100] (angle change of 1.0°)
[001]	parallel	[001]
$d(100) = 20.20$ Å		$d(010) = 20.36$ Å
$d(010) = 7.16$ Å		$d(100) = 7.16$ Å
$d(001) = 20.28$ Å		$2d(001) = 21.02$ Å

Investigation of Topotaxy. When the single crystals are heated, to ~105 °C, a violet reaction front can be observed advancing through the yellow crystals. The advance can be halted upon cooling, showing the transformation to be essentially irreversible, and subsequent single-crystal photographs show diffraction patterns of both compounds. While mosaicity of the violet component is not good (on Weissenberg photographs ~90% of the intensity is spread over ~7° in ω), the reaction is indisputably topotactic, in which, in all three dimensions, relationships can be established between a unit cell for the yellow dimer and a unit cell for the violet monomer. Since these photographs reproduce notoriously

(12) Waters, J. M.; Ibers, J. A. *Inorg. Chem.* **1977**, *16*, 3273–3277.

Table V. Final Atomic Parameters for $NiBr_2(dab)$[a]

atom	x	y	z	U_{11}	U_{12}	U_{13}	U_{12}	U_{13}	U_{23}
Ni	0.1956 (2)	0.08355 (6)	0.2348 (1)	1.03 (6)	2.10 (7)	2.45 (7)	−0.05 (6)	−0.30 (5)	−0.04 (6)
Br(1)	0.3180 (1)	0.07639 (6)	0.0274 (1)	2.10 (5)	3.45 (6)	2.55 (5)	0.25 (5)	0.26 (4)	0.11 (5)
Br(2)	0.3534 (1)	0.11998 (6)	0.4205 (1)	2.11 (5)	4.65 (7)	3.22 (5)	−0.38 (5)	−0.82 (4)	−1.14 (5)
N91)	−0.0619 (10)	0.1219 (4)	0.1912 (9)	1.05 (46)	2.44 (57)	2.33 (49)	−0.68 (42)	−0.23 (38)	0.06 (44)
N(2)	0.0527 (10)	−0.0028 (4)	0.2594 (6)	1.61 (41)	2.06 (45)	1.21 (37)	0.55 (35)	−0.22 (31)	0.19 (33)
C(1)	−0.1852 (12)	0.0757 (5)	0.2123 (9)	1.26 (46)	2.41 (57)	3.03 (53)	0.19 (45)	−0.82 (38)	0.33 (46)
C(2)	−0.1098 (12)	0.1945 (5)	0.1912 (9)	1.05 (46)	2.44 (57)	2.33 (49)	−0.68 (42)	−0.23 (38)	0.07 (44)
C(3)	0.0573 (14)	0.2289 (5)	0.1295 (11)	2.50 (57)	1.68 (59)	6.27 (77)	−0.36 (48)	1.53 (53)	1.03 (54)
C(4)	−0.1368 (16)	0.2249 (6)	0.3248 (10)	4.58 (69)	2.69 (65)	3.44 (60)	−0.12 (56)	−0.51 (53)	−0.59 (51)
C(5)	−0.2850 (14)	0.2047 (5)	0.1077 (10)	2.65 (57)	1.81 (57)	4.89 (66)	0.08 (46)	−2.30 (49)	0.99 (50)
C(6)	−0.1225 (13)	0.0060 (6)	0.2391 (9)	1.80 (54)	3.01 (63)	2.41 (50)	−0.01 (47)	−0.03 (41)	0.24 (46)
C(7)	0.1359 (13)	−0.0698 (5)	0.2951 (9)	2.44 (51)	1.79 (55)	3.14 (55)	0.08 (46)	0.63 (41)	0.01 (46)
C(8)	0.3263 (16)	−0.0742 (6)	0.2305 (11)	5.09 (75)	3.24 (69)	5.76 (77)	2.04 (60)	3.16 (64)	1.34 (60)
C(9)	0.0079 (17)	−0.1293 (6)	0.2567 (10)	5.49 (77)	3.46 (75)	3.96 (66)	0.43 (63)	−1.23 (56)	0.37 (57)
C(10)	0.1637 (14)	−0.0689 (6)	0.4418 (9)	3.10 (59)	3.61 (69)	2.90 (55)	0.48 (52)	−0.40 (45)	0.84 (51)

[a] See footnote to Table II

Table VIII. Bond Distances (Å) for Non-Hydrogen Atoms of $[NiBr_2(dab)]_2$ (I) and $NiBr_2(dab)$ (II)

	distance			distance	
atoms	I	II	atoms	I	II
Ni-Br(1)	2.4574 (9)	2.333 (2)	C(1)-C(6)	1.456 (8)	1.470 (13)
Ni-Br(2)	2.4966 (9)	2.343 (2)	C(2)-C(3)	1.508 (9)	1.521 (12)
Ni-Br(2)'[a]	2.5829 (9)		C(2)-C(4)	1.511 (11)	1.527 (13)
Ni-N(1)	2.042 (4)	1.996 (7)	C(2)-C(5)	1.491 (12)	1.523 (12)
Ni-N(2)	2.039 (4)	2.002 (8)	C(7)-C(8)	1.499 (10)	1.525 (13)
N(1)-C(1)	1.254 (6)	1.266 (12)	C(7)-C(9)	1.476 (14)	1.535 (15)
N(2)-C(6)	1.265 (6)	1.275 (11)	C(7)-C(10)	1.494 (12)	1.535 (13)
N(1)-C(2)	1.493 (7)	1.485 (12)			
N(2)-C(7)	1.488 (7)	1.492 (12)			

[a] Br(2)' and Br(2) are related by the symmetry operation ($^1/_2 - x$, $^1/_2 - y$, $-z$).

Table IX. Bond Angles (deg) among Non-Hydrogen Atoms for $[NiBr_2(dab)]_2$ (I) and $NiBr_2(dab)$ (II)

	angle			angle	
atoms	I	II	atoms	I	II
Br(1)-Ni-Br(2)	91.85 (3)	126.78 (6)	N(1)-C(1)-C(6)	117.4 (5)	117.8 (8)
Br(1)-Ni-N(1)	90.5 (19)	105.4 (2)	N(2)-C(6)-C(1)	119.0 (4)	116.9 (9)
Br(1)-Ni-N(2)	98.1 (1)	105.3 (2)	N(1)-C(2)-C(3)	108.8 (4)	108.0 (7)
Br(2)-Ni-N(1)	157.6 (1)	114.4 (2)	N(1)-C(2)-C(4)	107.6 (5)	106.4 (7)
Br(2)-Ni-N(2)	120.7 (1)	113.3 (2)	N(1)-C(2)-C(5)	109.8 (5)	113.1 (7)
N(1)-Ni-N(2)	80.8 (2)	82.5 (3)	N(2)-C(7)-C(8)	106.0 (4)	107.1 (8)
Br(2)'-Ni-Br(1)[a]	165.79 (3)		N(2)-C(7)-C(9)	105.8 (5)	112.4 (8)
Br(2)'-Ni-Br(2)	83.11 (3)		N(2)-C(7)-C(10)	113.5 (5)	106.3 (8)
Br(2)'-Ni-N(1)	89.2 (1)		C(3)-C(2)-C(4)	109.6 (6)	108.6 (8)
Br(2)'-Ni-N(2)	95.8 (1)		C(3)-C(2)-C(5)	111.2 (7)	109.9 (8)
Ni-N(1)-C(1)	112.0 (3)	111.2 (6)	C(4)-C(2)-C(5)	109.7 (6)	110.6 (8)
Ni-N(2)-C(6)	110.8 (3)	111.2 (7)	C(8)-C(7)-C(9)	109.9 (7)	111.8 (9)
Ni-N(1)-C(2)	128.5 (3)	126.2 (6)	C(8)-C(7)-C(10)	109.7 (7)	109.6 (6)
Ni-N(2)-C(7)	128.4 (3)	125.7 (6)	C(9)-C(7)-C(10)	111.7 (7)	109.5 (8)
C(2)-N(1)-C(1)	119.5 (4)	122.5 (8)			
C(7)-N(2)-C(6)	120.9 (4)	123.1 (8)			

[a] See footnote to Table VIII.

poorly, they are shown diagrammatically in Figure 1.

Unequivocal identification of the spots of the violet product was made by comparison to powder photographs and photographs of separately prepared single crystals. The relationships shown in Chart I were established by using the room-temperature unit cells that best displayed the symmetry of the crystal structures ($C2/c$ and $P2_1/n$).

Results and Discussion

$[NiBr_2(dab)]_2$ (I). Complex I comprises centrosymmetrically related dimers, as illustrated in Figure 2, and in Tables VIII and IX bond distances and bond angles are tabulated. The stereochemistry around the nickel atom can be viewed as a distorted trigonal bipyramid, with atoms Br(1), Ni, and Br(2)' forming the trigonal axis. The dimer also conforms rather closely in symmetry to a capped tetrahedron, where N(1)–N(2) and Br(1)–Br(2)' form orthogonal edges of a tetrahedron of D_{2d} symmetry and where Br(2) is positioned asymmetrically on the Br(2)'–Br(1)–N(2) face. The dimers are well separated and thus the moderately large thermal motions of many atoms are expected. Among non-hydrogen atoms there are no contacts closer than 3.3 Å and no hydrogen-non-hydrogen contacts closer than 3.0 Å; two H···H contacts of 2.29 Å occur while all others exceed 2.49 Å. The arrangement of dimers in the unit cell is illustrated in Figure 3.

In Table X selected metrical details for some related complexes are given.[13-18] Complex I is generally similar to $[NiBr_2(dmp)]_2$ except that the marked asymmetry in the bridging Ni–Br bonds of the latter[13] is considerably less.

$NiBr_2(dab)$ (II). Complex II is monomeric with a distorted $NiBr_2N_2$ tetrahedron of D_{2d} symmetry as illustrated in Figure 4,

(13) Butcher, R. J.; Sinn, E. *Inorg. Chem.* **1977**, *16*, 2334–2345.
(14) tom Dieck, H.; Svoboda, M.; Kopf, J. *Z. Naturforsch., B* **1978**, *B33*, 1381–1385.
(15) Preston, H. S.; Kennard, C. H. L. *J. Chem. Soc. A* **1969**, 2682–2685.
(16) Long, G. J.; Schlemper, E. O. *Inorg. Chem.* **1974**, *13*, 279–284.
(17) Jansen, J. C.; van Koningsveld, H.; van Ooijen, J. A. C.; Reedijk, J. *Inorg. Chem.* **1980**, *19*, 170–174.
(18) Phelps, D. W.; Goodman, W. H.; Hodgson, D. J. *Inorg. Chem.* **1976**, *15*, 2266–2270.

Table X. Selected Dimeric NiX_2N_2 Complexes[a]

	Ni-X_{ter}	Ni-X_{br}	Ni-N	Ni···Ni	X···X	X_{br}-Ni-X_{br}'	N-Ni-N	geometry[b]
$[NiBr_2(dab)]_2$	2.457 (1)	2.497 (1) 2.583 (1)	2.039 (4) 2.042 (4)	3.801	3.372	83.11 (3)	80.8 (2)	dtp[b]
$[NiBr_2(dmp)]_2$[c]	2.458 (1)	2.468 (1) 2.649 (1)	2.021 (2) 2.034 (2)	3.826	3.402	83.26 (1)	82.44 (8)	dtp
$[NiBr(dab_1)]_2$[d]		2.444 (3) 2.447 (4)	1.95 (2) 1.91 (2)	3.460	3.455	89.9 (2)	83.1 (8)	dt
$[NiCl_2(biq)]_2$[e]	2.306 (1)	2.372 (1) 2.400 (1)	2.034 (1) 2.042 (2)	3.563	3.172	83.32 (2)	80.37 (6)	dtp
$[NiCl_2(dmp)]$[f]	2.307 (1)	2.378 (1) 2.414 (1)	2.033 (2) 2.049 (2)	3.600	3.162	82.6 (1)	82.00 (7)	dtp
$[NiCl_2(dmp)]_2$[g]	2.316 (3)	2.378 (3) 2.384 (3)	2.06 (2) 2.07 (2)	3.602	3.121	81.9 (1)	81.7 (4)	dtp
$[NiCl_2(Qnqn)]_2$[h]	2.296 (2)	2.408 (2) 2.422 (2)	2.047 (3) 2.067 (2)	3.652	3.162	81.78 (6)	97.6 (1)	dsp
$[NiCl_2(dmpz)]_2$[i]	2.318 (1)	2.319 (1) 2.456 (1)	2.033 (3) 2.099 (3)	3.587	3.154	82.64 (4)	87.6 (1)	dtp
$[CuBr_2(dmen)]_2$[j]	2.401 (1)	2.463 (2) 2.868 (2)		3.570				dsp

[a] Distances in Å; angles in deg. [b] dtp = distorted trigonal bipyramidal with X_{br}-Ni-X_{ter} as the trigonal axis. For most, distorted square pyramidal (dsp) is equally applicable, in which case an N atom forms the apex; dt = distorted tetrahedra. [c] dmp = 2,9-dimethyl-1,10-phenanthroline. Reference 13. [d] dab_1 = di-*N*,*N*'-(2,4-dimethyl-3-pentyl)diazabutadiene. Note Ni(I) complex. Reference 14. [e] biq = 2,2'-biquinolyl. Reference 13. [f] Reference 13. [g] Chloroform solvate $[NiCl_2(dmp)]_2 \cdot 2CHCl_3$. Reference 15. [h] Qnqn = *trans*-2-[(2'-Quinolyl)methylene]-3-quinuclidine. Reference 16. [i] dmpz = Bis(3,5-dimethylpyrazolyl). Note Cl'-Ni-N forms the trigonal axis. Reference 17. [j] dmen = *N*,*N*-dimethylethylenediamine. Reference 18.

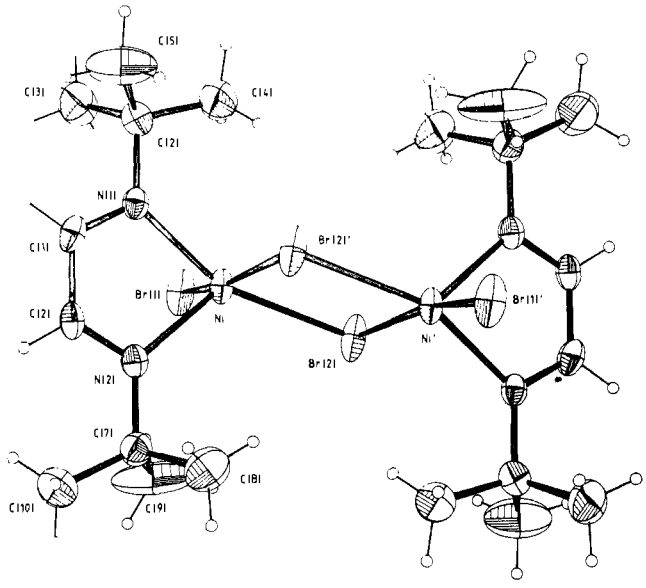

Figure 2. Molecular diagram of $NiBr_2(dab)$ dimers. The atom-labeling scheme is defined. Thermal ellipsoids are drawn at the 30% probability level. Hydrogen atoms are shown artificially small.

and in Tables VIII and IX bond distances and bond angles are tabulated. Despite the less crowded environment, the bite of the diazabutadiene ligand increases by only 1.7 (4)°, indicating considerable stereochemical rigidity in this ligand. As expected all Ni–ligand separations decrease relative to the five-coordinate dimer, especially the Ni–Br separations. The monomers are well separated, with no contacts among non-hydrogen atoms closer than 3.55 Å; among non-hydrogen–hydrogen atoms none are closer than 2.80 Å, and among hydrogen atoms none are closer than 2.42 Å. Figure 5 shows the crystal packing arrangement.

In Table XI selected metrical details for some related complexes[13,19] are presented. Bond parameters for the two bromo monomer complexes are in close accord. No monomeric $NiCl_2N_2$ complexes appear to have been completely characterized.[20,21] Substitution of iodo for bromo ligands leads to only marginally shorter Ni–N bond lengths, analogous to that for the bromo and chloro dimers.

Table XI. Selected Monomeric NiX_2N_2 Complexes[a]

	$NiBr_2(dab)$	$NiBr_2(biq)$[b]	$NiI_2(dmp)$[c]	$NiI_2(bc)$[d]
Ni-X	2.333 (2) 2.343 (2)	2.331 (1) 2.351 (1)	2.530 (1) 2.546 (1)	2.497 (1) 2.515 (1)
Ni-N	1.996 (7) 2.002 (8)	1.991 (5) 1.993 (5)	1.987 (3) 2.005 (3)	1.981 (4) 1.983 (4)
N-Ni-N	82.5 (3)	82.6 (2)	83.8 (1)	83.2 (2)
X-Ni-X	126.78 (6)	124.94 (4)	126.75 (2)	132.04 (3)

[a] See footnotes to Table X. [b] Reference 13. [c] Reference 18. [d] bc = 2,9-dimethyl-4,7-diphenyl-1,10-phenanthroline (bathocuproine). Reference 19.

Influence on the Geometry of NiX_2N_2 Complexes. Bonding is always a compromise between maximum orbital overlap and minimum destabilizing nonbonded ligand–ligand interactions. It is usually difficult to assign horse and cart to these opposing effects in discussing stereochemical trends among related complexes. Nonetheless, we are unconvinced that the asymmetry observed in the Ni-X_{br} bonds of the dimeric complexes is primarily attributable to nonbonded interactions between the bidentate ligand and the halo groups, as has been advanced by several groups.[13,17] Considering first the complexes where the pseudotrigonal axis is defined by the X'_{br}-Ni-X_{ter} moiety, we note that the X_{br}-Ni-N bond angles are markedly asymmetrical—typically ~125° and ~155°.[21] Intramolecular steric interactions between the halo and nitrogenous bidentate ligands would be ameliorated if the dab ligand adopted a more symmetrical conformation. Comparison of $[NiBr_2(dab)]_2$ and its phenanthroline analogue, $[NiBr_2(dmp)]_2$, reveals that the former species displays greater asymmetry in its Br_{br}-Ni-N bond angles but less asymmetry in the Ni-Br_{br} bond lengths. Second, for the $NiCl_2(dmpz)]_2$ dimer,[17] which exhibits much greater asymmetry in the Ni-Cl_{br} bond lengths than its analogues, the trigonal axis is defined by the N-Ni-Cl_{br}' group. Of the compounds listed in Table X, this conforms most closely to trigonal-bipyramidal geometry.[22] Here one can reasonably ascribe the long Ni-C_{br} bond to a trans effect exerted by the tightly coordinated nitrogen ligand. Moreover, in the $NiCl_2(dmp)$ system[15] there exists a monomeric five-coordinate aquo species $NiCl_2(OH_2)(dmp)$ whose structure is distorted trigonal bipyramidal with a difference of 0.25 Å in the Ni-N bonds.[23,24] In

(19) Butcher, R. J.; O'Connor, C. J.; Sinn, E. *Inorg. Chem.* **1979**, *18*, 492–497.
(20) A purple $NiCl_2(dmp)$ species isomorphous by X-ray powder photography with the tetrahedral $ZnCl_2(dmp)$ species has been isolated.[21]
(21) Preston, H. S.; Kennard, C. H. L. *J. Chem. Soc. A* **1969**, 1956–1961.
(22) Indeed, these dimers could be viewed as octahedral complexes with a single vacant coordination site.

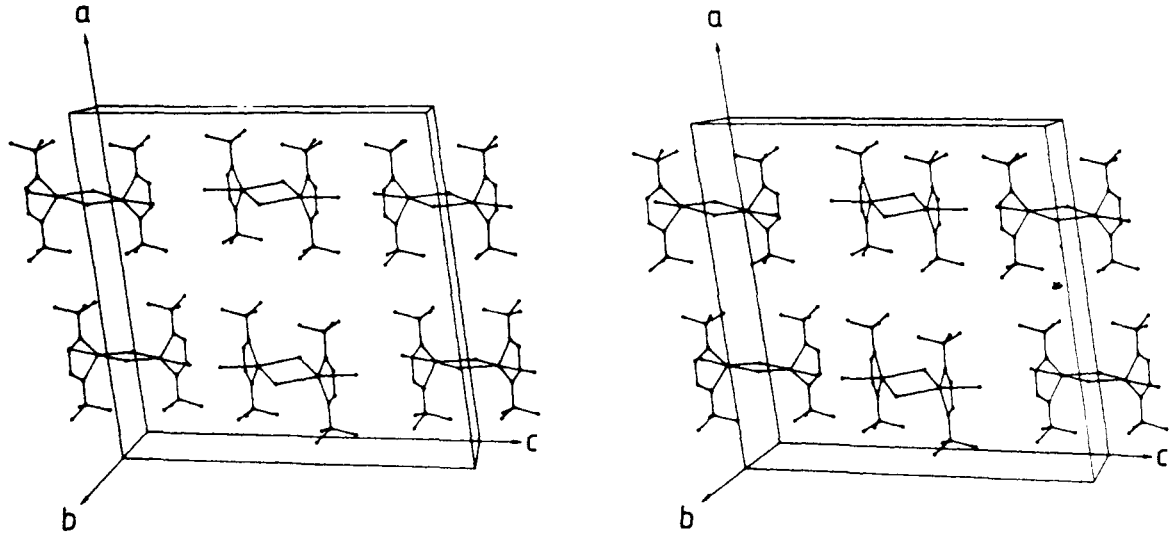

Figure 3. Diagram illustrating the packing of $[NiBr_2(dab)]_2$ in the unit cell.

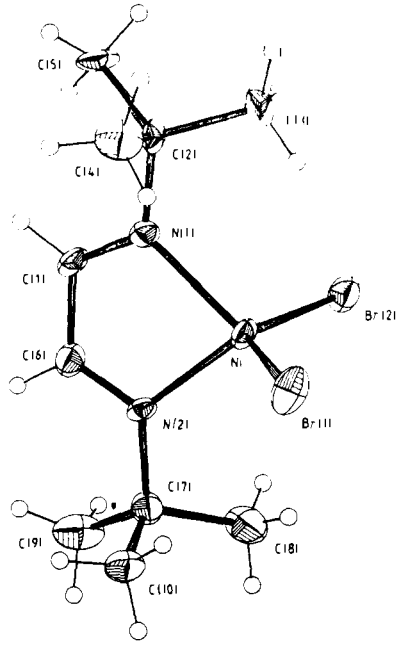

Figure 4. Molecular diagram of $NiBr_2(dab)$ monomer. The atom-labeling scheme is shown. Thermal ellipsoids are drawn at the 40% probability level. Hydrogen atoms are shown artifically small.

addition, a number of dimeric five-coordinate copper(II) complexes are known,[18,25-28] a representative example of which[18] has been included in Table X. Highly asymmetric $Cu-X_{br}$ separations ($\Delta > 0.4$ Å) are observed here for both chloro and bromo complexes, indicating still greater tendency toward four-coordination than is observed in the dimeric $NiBrN_2$ species. Finally, for zinc(II) only the tetrahedral geometry is found, as in $ZnCl_2(dmp)$.[21] Within the NiX_2N_2 system the tendency of chloro derivatives to adopt five-coordination with symmetrical $Ni-Cl_{br}$ separations, of bromo derivatives to adopt five-coordination with asymmetrical $Ni-Br_{br}$ separations or tetrahedral four-coordination, and of iodo derivatives to adopt exclusively four-coordination has been noted previously.[13] Thus we conclude that the asymmetry in bridging metal-halo bonds reflects in the main coordination preferences of the metal center rather than intramolecular interactions between coordinated ligands and noncoordinated atoms of the bidentate group.

Structural Changes and the Topotactic Transformation. By themselves the unit cell relationships described earlier provided little information on the atomic nature of the structural changes; however, they do provide a useful framework within which structural changes can be analyzed. The product of this solid-state reaction, if conducted in an isotropic environment, is expected to be twinned with $[100]_{monomer}$ nonuniquely defined with respect to $[010]_{dimer}$. However, the change in angle, $\pm(91.03 - 90°) = \pm 1.0°$, is much smaller than the mosaic spread and/or coherence length, and therefore twinning, it it occurs, is not observable in the X-ray diffraction studies. In the $NiBr_2[P(CH_2CH_2CN)_3]_2$ system,[3d] where the transformation was from orthorhombic to monoclinic, twinning was not observed when the reaction began on a single face of the crystal. In Figure 6 the unit cells are shown, minus the clarity-obscuring *tert*-butyl groups, in orientations that reflect the topotactic relationships. The direction of propagation of the boundary between the yellow (dimer) and violet (monomer) phases is fastest parallel to $[010]_{dimer}$; in the directions $[100]_{dimer}$ and $[001]_{dimer}$ no significant difference was observed. Furthermore, electron microscopy of single crystals and partly reacted powdered samples and conventional analysis of the kinetic data[29] are also consistent with a concerted three-dimensional propagation of phase boundaries, as opposed to a renucleation phenomenon for the reaction. Thus we are justified in presenting for this topotactic reaction a detailed mapping relating the $NiBr_2(dab)$ units of the dimer to the monomer. We assume that the route of lowest "activation energy" involves (1) the breakage of the minimum number of bonds and (2) the smallest movement of atoms consistent with avoiding steric clash of molecular fragments. It is clear then that this reaction proceeds in two well-defined steps: first, breakage of the longer weaker Ni-Br(2)′ bond and second, concerted movement of the monomeric units concomitant with rearrangement to D_{2d} geometry.

Figures 3 and 5, but no Figure 6, show that a 180° rotation of the $NiBr_2(dab)$ monomers with their bulky *tert*-butyl groups can be discounted, especially since the product crystal structure is highly oriented with respect to that for the starting material. Each monomer unit moves on the order of 5 Å as the Ni···Ni′ separation changes from 3.801 Å in the centrosymmetrically related dimer to 9.893 Å in the product, where a 2_1 screw axis now relates these units. It is the loss of this inversion center *within* dimers that leads to a halving of the unit cell in the violet product and a disappearance of the *C* center. The monomeric components of dimers related by *C*-centering move in opposite directions. The

(23) A similar species is possible for the decomposition of $[NiBr_2(dab)]_2$ and $NiBr_2(dab)$ by atmospheric moisture.
(24) Preston, H. S.; Kennard, C. H. L. *J. Chem. Soc. A* **1969**, 2955-2958.
(25) Endres, H. *Acta Crystallogr., Sect. B* **1978**, *B34*, 3736-3739 and references therein.
(26) Wilson, R. B.; Hatfield, W. E.; Hodgson, D. J. *Inorg. Chem.* **1976**, *15*, 1712-1716.
(27) Svedung, D. H. *Acta Chem. Scand.* **1969**, *23*, 2865-2878.
(28) Sletten, E.; Apeland, A. *Acta Crystallogr., Sect. B* **1975**, *B31*, 2019-2022.
(29) Beer, H. R. PhD Dissertation, University of Zürich, 1982.

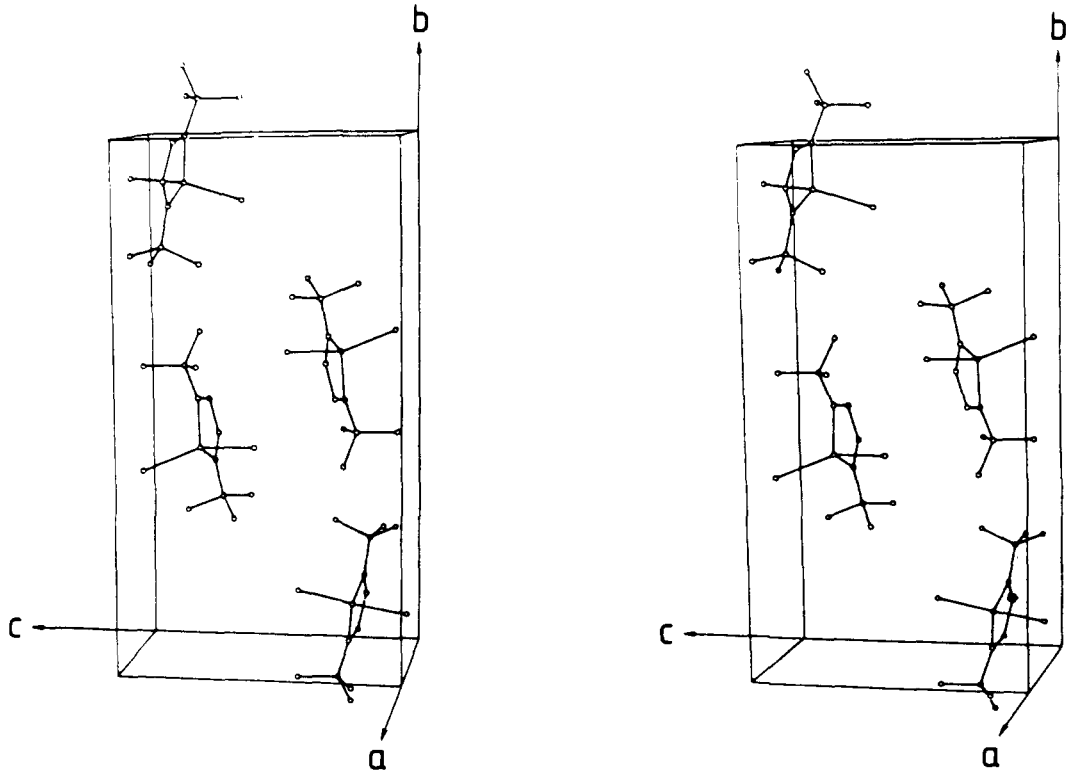

Figure 5. Diagram illustrating the packing of $NiBr_2$(dab) in the unit cell.

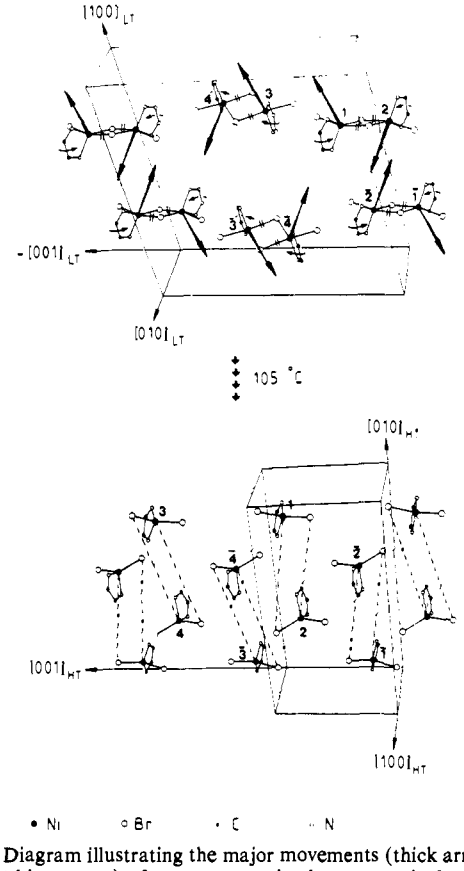

Figure 6. Diagram illustrating the major movements (thick arrows) and rotations (thin arrows) of atom groups in the topotactic formation of $NiBr_2$(dab).

centers of inversion *between* dimers are thereby retained; this, together with the new 2_1 axis, determines the space group symmetry $P2_1/n$ of the product.

Substantial rotation (~25°) of the diazabutadiene occurs relative to the $NiBr_2$ moiety, which also adjusts to a smaller Br–Ni–Br angle, to give a symmetrical (D_{2d}) $NiBr_2$(dab) unit. The effect of this is to render the diazabutadiene planes in the violet phase approximately parallel to (001) product. These changes are summarized in Figure 6. The movements of atoms observed here are, we believe, unprecedentedly large for a transformation that is highly topotactic or in the notation of Cheng and Foxman, "triply specific".[3d] Despite intensive inspection of three-dimensional models of the crystal structures of the dimer and monomer, we could deduce no other plausible reaction mechanism.

A possibility similar transformation has been observed for the yellow dimeric $[NiCl_2(Qnqn)]_2$ complex at ~200 °C,[6f] but no mention was made as to whether this transformation proceeded in the geometrically and crystallographically specific way observed for $[NiBr(dab)]_2$. Whereas we observed no transformation of the violet form back to the yellow form even down to −150 °C, the temperature at which we collected data, Long et al. observed such a reversal at ~−80 °C.

It must be noted that the factors, both intrinsic (e.g., crystal quality and habit) and extrinsic (e.g., experimental conditions) that predispose a compound to undergo solid-state processes that lead to an oriented product rather than to amorphous or randomly oriented microcrystalline material, are far from understood; in some systems, despite apparently small changes in molecular shape and packing and retention of space group symmetry, the product of the solid-state process is randomly oriented with respect to the parent material.[30]

Acknowledgment. The support of the Swiss National Science Foundation is gratefully acknowledged.

Registry No. I, 75923-96-5; II, 73946-15-3; dab, 30834-74-3; dibromo(dimethoxyethane)nickel, 28923-39-9; glyoxal, 107-22-2; *tert*-butylamine, 75-64-9.

Supplementary Material Available: Listings of hydrogen atom parameters and $10|F_o|$ vs. $10|F_c|$ for $[NiBr_2(dab)]_2$ (Tables III and IV) and $NiBr_2$(dab) (Tables VI and VII) (38 pages). Ordering information is given on any current masthead page.

(30) For example: Cohen, M. D.; Coppens, P.; Schmidt, G. M. J. *J. Phys. Chem. Solids* **1964**, *25*, 258–260.